

## Quantitative Intramolecular Singlet Fission in Bipentacenes

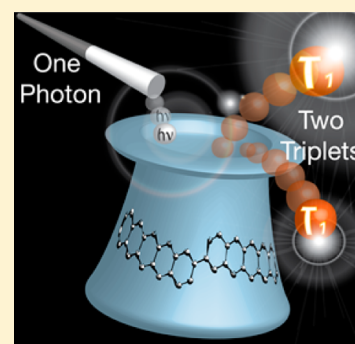
Samuel N. Sanders,<sup>†</sup> Elango Kumarasamy,<sup>†</sup> Andrew B. Pun,<sup>†</sup> M. Tuan Trinh,<sup>†</sup> Bonnie Choi,<sup>†</sup> Jianlong Xia,<sup>†,||</sup> Elliot J. Taffet,<sup>†</sup> Jonathan Z. Low,<sup>†</sup> John R. Miller,<sup>‡</sup> Xavier Roy,<sup>†</sup> X.-Y. Zhu,<sup>†</sup> Michael L. Steigerwald,<sup>\*,†</sup> Matthew Y. Sfeir,<sup>\*,§</sup> and Luis M. Campos<sup>\*,†</sup>

<sup>†</sup>Department of Chemistry, Columbia University, New York, New York 10027, United States

<sup>‡</sup>Department of Chemistry and <sup>§</sup>Center for Functional Nanomaterials, Brookhaven National Laboratory, Upton, New York 11973, United States

### Supporting Information

**ABSTRACT:** Singlet fission (SF) has the potential to significantly enhance the photocurrent in single-junction solar cells and thus raise the power conversion efficiency from the Shockley–Queisser limit of 33% to 44%. Until now, quantitative SF yield at room temperature has been observed only in crystalline solids or aggregates of oligoacenes. Here, we employ transient absorption spectroscopy, ultrafast photoluminescence spectroscopy, and triplet photosensitization to demonstrate intramolecular singlet fission (iSF) with triplet yields approaching 200% per absorbed photon in a series of bipentacenes. Crucially, in dilute solution of these systems, SF does not depend on intermolecular interactions. Instead, SF is an intrinsic property of the molecules, with both the fission rate and resulting triplet lifetime determined by the degree of electronic coupling between covalently linked pentacene molecules. We found that the triplet pair lifetime can be as short as 0.5 ns but can be extended up to 270 ns.



### INTRODUCTION

The third generation of solar cells is based on materials that operate by nonconventional photophysical mechanisms to overcome the Shockley–Queisser limit.<sup>1–3</sup> In molecules and polymers, singlet fission (SF) is the process whereby two triplets are generated from a single photon.<sup>4</sup> Devices fabricated from singlet fission molecules have exceeded 100% external quantum efficiency,<sup>5,6</sup> but many fundamental challenges remain: (a) there are a limited number of materials that undergo SF; (b) appropriate heterojunctions must be engineered to extract the multiple excitons; and (c) device architectures that exploit SF must be engineered. While the resurgent interest in SF has been catalyzed by solar cells, multiexcitonic materials can also be widely applicable in other optoelectronic thin-film technologies, such as photodetectors.<sup>7</sup>

The lack of a variety of chromophores that undergo SF independently of intermolecular interactions is a major hurdle to the development of multiexcitonic devices. For example, acenes can undergo SF only when neighboring chromophores are electronically coupled in the solid state or by diffusional collisions in highly concentrated solutions. We refer to this process as intermolecular singlet fission (xSF),<sup>5,7–12</sup> where pentacene has surfaced as the prototypical material since its SF triplet quantum yield is quantitative (200%).<sup>10</sup> In fact, even in crystalline media, the crystal packing and morphology have a significant effect on SF rates, rendering practical applications more challenging.<sup>13–16</sup> A more suitable approach is to employ intramolecular singlet fission (iSF) active layers, but iSF has rarely been observed in organic materials, with yields before

2015 languishing below 30% and/or as an activated process.<sup>17–19</sup>

We have recently pioneered the design of organic materials based on strong-donor/strong-acceptor copolymers and small molecules that facilitate iSF through a photoexcited state with strong charge-transfer (CT) character, exhibiting up to 170% triplet yield in a polymer.<sup>20,21</sup> Such design principles were founded on the CT-mediated mechanism of xSF. Interestingly, there is another strategy in molecular materials, which involves the covalent coupling of two xSF chromophores. As of 2014, several groups attempted to model and synthesize such dimers based on tetracene and diphenylisobenzofuran, only to find low experimental triplet yields (<10%).<sup>22–27</sup> However, it can be possible to improve the yields by using covalently coupled pentacene dimers and by understanding how the conjugation within these chromophores affects iSF.

During the course of revisions to this paper, Zirzmeier et al.<sup>28</sup> reported a pentacene dimer that exhibits 156% yield of triplets, along with two other dimers of the same family. Such dimers are coupled through the 6-position by *o*-, *m*-, and *p*-diethynylbenzene, concomitantly varying both through-bond and through-space interactions between the pentacenes. While the ethynyl groups impart stability, we envisioned that coupling through the 2-position would yield a modular platform to fine-tune structural components that evade through-space interactions between the pentacenes, thus focusing on through-bond coupling as a function of distance (Figure 1). In this vein, we

Received: December 16, 2014

Published: June 23, 2015

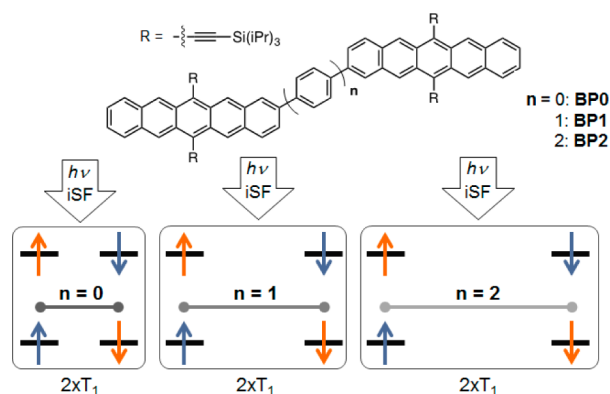


**Figure 1.** Pentacene chromophores of interest, where both are directly coupled ( $n = 0$ , **BP0**), and separated by one ( $n = 1$ , **BP1**) or two ( $n = 2$ , **BP2**) phenylene groups, which affect the triplet spectra, as well as the rates of fission and recombination.

synthesized a series of singlet fission dimers by coupling pentacenes at the 2,2'-position with and without (oligo)phenylene spacers. Using these spacers, we can vary the proximity and extent of conjugation of the pentacenes, which allows for control of the rate of singlet fission and the rate of recombination of the two triplets. The ability to extend the lifetime of the triplet pair ( $2xT_1$ ) is a major challenge in multiexcitonic devices based on iSF chromophores, where efficient charge extraction is essential for the overall performance of devices.

Here, we report soluble, stable derivatives of 2,2'-bipentacene that exhibit the maximum iSF yield,  $\sim 200\%$ , via an intramolecular process on isolated molecules. We find that the singlet fission rate and triplet lifetimes can be tuned by varying the length of the spacer group. While the connectivity of the pentacenes in the reported dimers is similar to that of tetracene dimers previously proposed,<sup>29</sup> the chromophores in Figure 1 have key distinctions: (a) since xSF in pentacene is known to be exothermic, covalently coupling two pentacenes can lead to a similarly energetically favored iSF process that stems from a delocalized singlet (in apparent contrast to localized singlets observed by Zirzmeier et al.<sup>28</sup>); and (b) triisopropylsilylacetylene (TIPS) groups render the product soluble and stable, resulting in facile and scalable synthesis.<sup>30</sup>

## RESULTS AND DISCUSSION

In singlet fission, the singlet state evolves into a spin-correlated triplet pair, also called a multiexcitonic state, which dephases into two individual triplets ( $2xT_1$ ).<sup>31</sup> In order for SF to take place, the energy of the singlet state must be approximately twice the energy of the triplet. Using a method similar to that of Greyson et al.<sup>29</sup> (Supporting Information), we calculated the energy of the singlet to be roughly isothermic with two triplets for all three bipentacenes discussed. Satisfaction of the energetic requirement  $2E(T_1) \leq E(S_1)$ , within the margin of error for density functional theory (DFT) energy calculations, suggests that these compounds are feasible candidates for iSF. Furthermore, DFT simulations, using the optimized  $S_0$  ground state, reveal that the highest occupied and lowest unoccupied molecular orbitals (HOMO and LUMO, respectively) of the  $S_0$  state are delocalized over the entire molecule (Figures SIV.1, SIV.3, and SIV.5, Supporting Information). The lowest-energy excited singlet state,  $S_1$ , is optically allowed and in all three cases results primarily from the expected electronic excitation,

viz., moving an electron from the  $S_0$  HOMO to the  $S_0$  LUMO (further details in Supporting Information). Independent DFT calculations on the lowest-energy triplet,  $T_1$ , performed from the same optimized  $S_0$  geometry, show that the two singly occupied orbitals that characterize  $T_1$  are localized on just one of the pentacene subunits in all three molecules. This localization is not surprising as it maximizes the stabilizing exchange interaction. The localization of  $T_1$  suggests that the electronic structure of these molecules is appropriate to accommodate a second “isolated” triplet produced via iSF.

Steady-state absorption spectra of **BP0**, **BP1**, and **BP2** in chloroform are compared to that of a single pentacene chromophore, TIPS-pentacene (**TPc**), in Figure 2. The low-

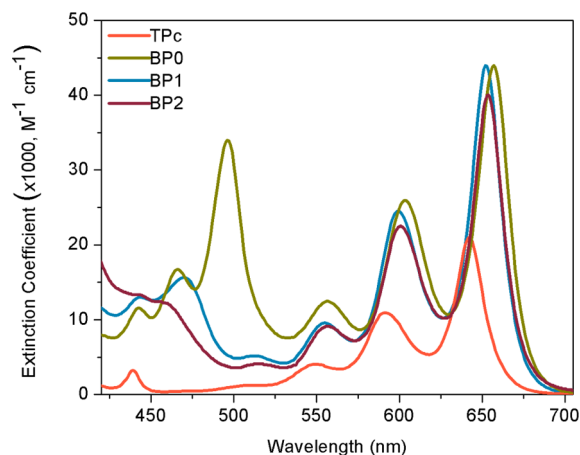


**Figure 2.** Comparison of **TPc** spectrum with UV-vis spectra of pentacene dimers with 0, 1, and 2 *p*-phenylene spacers (**BP0**, **BP1**, and **BP2**, respectively).

energy region of the spectrum is qualitatively similar and red-shifted by approximately 50 meV in all bipentacenes. Additionally, a new set of high-energy peaks appears in **BP0**, broadening the absorption to include a greater portion of the visible spectrum. This feature is unique to the connectivity of these molecules, and is not observed in other oligopentacene derivatives.<sup>32</sup> We found that the bipentacene series all have molar extinction coefficients roughly twice that of **TPc**. Finally, concentration-dependence studies on all bipentacenes indicate no aggregation, which is typically manifested as a red shift in the absorption spectrum (Figures SIII.1–4, Supporting Information).<sup>33</sup> Similarly, the dependence of signal intensity on concentration adheres to Beer's law (Figure SIII.2, Supporting Information). The lack of aggregates is important to ensure that the photophysical measurements are probing molecules that are fully dissolved, and intermolecular coupling effects are not playing a role in the dynamics of the excited state.

In order to evaluate and compare the photophysical dynamics of the materials, we first describe our observations of **BP0**, and we then proceed to compare the results to **BP1** and **BP2**. The key focus is to understand the effects of pentacene proximity on the mechanism of iSF. This relationship is probed by modulating the length of conjugated phenylene spacers. As shown in Figure 1, we postulate that the decreasing proximity of triplet sites from **BP0** to **BP1** and to **BP2** will drastically affect the rates of iSF and triplet-triplet recombination, as well as the triplet spectra.

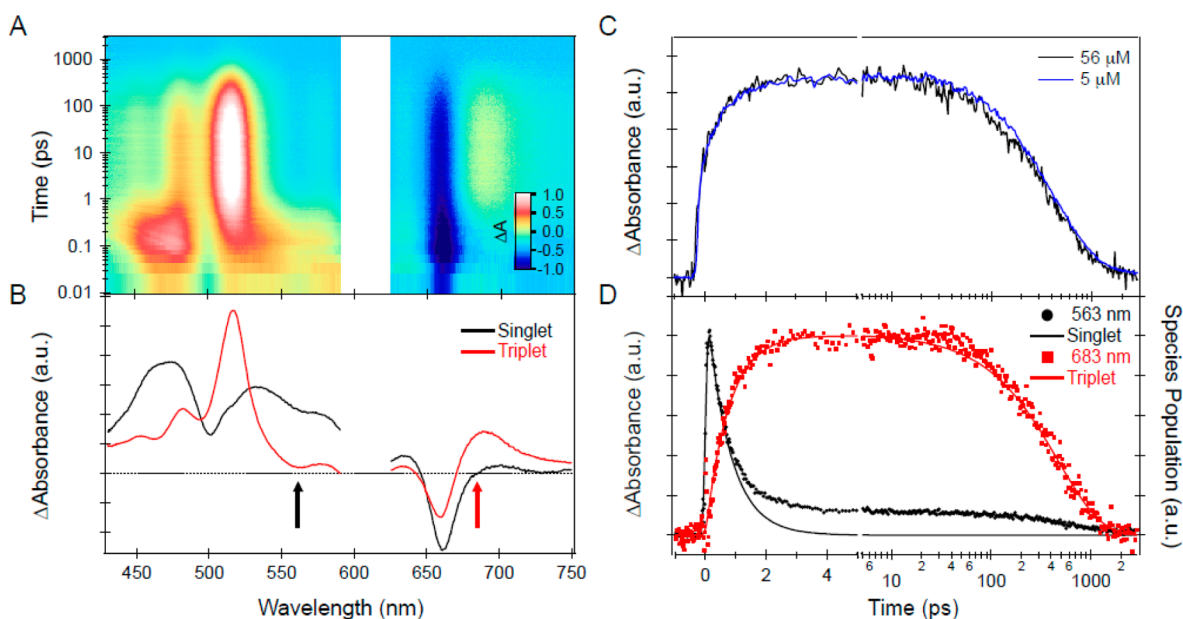


**Figure 3.** (A) Normalized transient absorption data of **BPO** in chloroform ( $56 \mu\text{M}$ ,  $600 \text{ nm}$  pump). Due to pump wavelength scatter, small portions of the data have been excluded for clarity. (B) Deconvoluted transient spectra of singlet and triplet species as solved by global analysis (details in Supporting Information). It should be noted that differences in the magnitude of bleach in panel B are attributable to overlap with the triplet spectrum, not to a reduction in bleach. (C) Normalized spectral slice at  $517 \text{ nm}$  showing that the carrier dynamics are independent of concentration over an order of magnitude. (D) Population evolution from global analysis is compared to raw data at wavelengths where primarily singlet ( $563 \text{ nm}$ , black arrow in panel B) and triplet ( $683 \text{ nm}$ , red arrow in panel B) dynamics are observed. The discrepancy at  $563 \text{ nm}$  is due to the  $\sim 20\%$  overlap with a triplet photoinduced absorption feature. Direct fits of the data are found in Figure SI.1 (Supporting Information).

Employing ultrafast transient absorption spectroscopy (TAS), we observed a rapid conversion of photoexcited singlets into triplets, occurring on a subpicosecond time scale in **BPO**. These two distinct populations can be clearly seen in 2D pseudocolor ( $\Delta A$ ) plots of transient absorption spectra as a function of probe wavelength and delay time (Figure 3A). Notably, the photoinduced absorption (PIA) features at  $470$  and  $560 \text{ nm}$  rapidly evolve into a new feature at  $517 \text{ nm}$ . The amplitude of the feature at  $517 \text{ nm}$  rises for a few picoseconds and then decays with a several hundred picosecond time constant back to the ground state (Figure 3C), during which the shape of the transient spectra remain constant. The negative feature at  $660 \text{ nm}$  persists for the duration of the conversion from singlet to triplet; it results from ground-state bleaching of the lowest energy optical transition that can be seen in the linear absorption spectrum (Figure 2).

On the basis of sensitization experiments along with the known TAS of **TPc** and related compounds, we assign the features that decay on the subpicosecond time scale to the singlet state and the slowly decaying features to the triplet state.<sup>8</sup> The triplet spectrum can be clearly isolated at times  $>5 \text{ ps}$ , when features associated with the singlet manifold have decayed. However, to isolate the rapidly decaying singlet features and get an accurate time scale for singlet fission, we use global analysis methods with a sequential kinetic decay model ( $S_1 \rightarrow 2xT_1 \rightarrow S_0$ ).<sup>34</sup> The deconvoluted spectra that result from global analysis are shown in Figure 3B, and the resulting species concentration profiles as a function of time are shown in Figure 3D (solid lines). We note that a triplet PIA feature overlaps spectrally with the position of the ground-state bleach. As a result, the ground-state recovery does not strictly correlate with the net magnitude of the bleach feature as a function of time. In other words, the net change in the bleach during the singlet decay is primarily due to the rise of the overlapping triplet PIA

and not due to the loss of excited-state population. However, after accounting for the nonzero baseline, we find that the overall ground-state bleach signal is conserved during the singlet fission process (details in Supporting Information), a signature of quantitative conversion of singlets to triplets.

Global analysis yields a time constant for singlet decay and concomitant triplet rise of  $760 \text{ fs}$ . From spectral deconvolution, we identify regions in the unprocessed data where the singlet ( $563 \text{ nm}$ ) and the triplet ( $683 \text{ nm}$ ) can be preferentially observed. We note that these regions do not correspond to the peaks of the singlet and triplet PIA features. The extracted raw kinetic traces at these wavelengths are compared against the computed population profiles (Figure 3D), and good agreement is found with our model that correlates the rise of the triplet with the decay of the singlet. Similarly, the data at both wavelengths fit well with a common set of time constants that agree with those determined from global fitting (Figure SI.1, Supporting Information).

The fast decay of the singlet excitons was further confirmed by time-resolved ultrafast photoluminescence spectroscopy (UFPL; details in Experimental Section). Photoluminescence is spin-allowed for singlet excitons but spin-forbidden for triplets. Therefore, the conversion of a singlet into two triplets observed in TAS corresponds to conversion from an emissive (singlet) to nonemissive (two triplet) state in the time-resolved UFPL experiment. A time constant of  $\sim 0.7 \text{ ps}$  for decay of the photoluminescence is extracted by fitting the time-resolved emission signal measured at  $675 \text{ nm}$ , near the peak of the photoluminescence spectrum (Figure 4A). The subpicosecond time constant for the decay of the singlet is in excellent agreement with transient absorption measurements, and taken together, these data support the assignment of quantitative, ultrafast, intramolecular singlet fission of a singlet exciton into two triplet excitons. We note that the emission lifetime in **TPc**

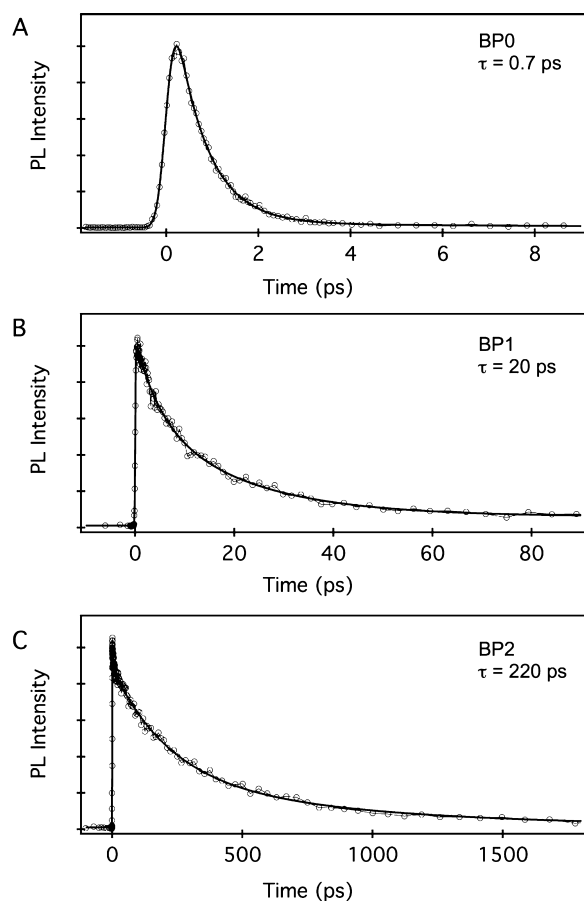


**Figure 4.** Ultrafast photoluminescence (UFPL) decay lifetimes ( $\tau$ ) of the emissive singlet state in (A) **BP0**, (B) **BP1**, and (C) **BP2**.

is  $>10$  ns, more than 4 orders of magnitude longer than what is observed in **BP0**.<sup>33</sup> A small fraction ( $\sim 3\%$  of the overall amplitude) of longer-lived emission is observed that could originate from trace monomer in our sample.

Since triplet pairs created via intramolecular singlet fission in solution are confined to a single molecule and are unable to diffuse apart intermolecularly (as in the case of xSF), the triplet recombination dynamics are faster than those resulting from typical intermolecular fission processes in the solid state. From transient absorption measurements (Figure 3), we determine that the triplet pair lifetime is  $\sim 450$  ps in **BP0**, compared to  $>100$  ns in pentacene crystals.<sup>35</sup> Furthermore, we can confirm that the observed subnanosecond lifetime is not the intrinsic lifetime of an individual triplet; since iSF occurs in dilute solution, we can utilize triplet sensitization techniques to directly compare the  $T_1$  versus  $2xT_1$  relaxation dynamics in **BP0** molecules.

Having obtained rates of singlet decay followed by population of the  $2xT_1$  state, the absorption features of the triplet pairs must be compared to the single-triplet spectrum obtained through sensitization. The process involves photoexcitation of anthracene, which undergoes intersystem crossing and subsequently transfers an electron via diffusive collisions to the **BP** chromophores.<sup>20,36,37</sup> The absorption spectrum of the triplet transient is recorded and compared to the  $2xT_1$  generated by singlet fission (Figure 5A). Interestingly, a subtle difference in the spectra is observed between individual triplets produced via sensitization and triplet pairs produced via singlet fission in **BP0**. This is evident in the feature at  $\sim 680$  nm. The

low-energy PIA feature (typically assigned to  $T_1 \rightarrow T_2$ ) is red-shifted by  $\sim 200$  meV in the sensitization experiment, though much better agreement is seen in the higher energy ( $T_1 \rightarrow T_3$ ) triplet PIA feature. This difference will be further discussed later, in comparison to the other two chromophores. The most striking difference between the individual triplet and the triplet pair state is observed in the decay time scale of triplet pairs ( $\sim 450$  ps), which is more than 4 orders of magnitude faster than that of individual triplets ( $>18 \mu\text{s}$ , Figure 5D). This ultrafast time scale is in agreement with recent reports of fast triplet–triplet recombination, resulting from the iSF process.<sup>20,28</sup> We note that the formation and decay kinetics of the  $2xT_1$  state have weak dependence on solvent (Supporting Information), distinct from other fast singlet deactivation processes that have been observed in conjugated small-molecule systems, such as intramolecular charge transfer.<sup>38–41</sup>

In **BP0**, fast triplet–triplet recombination and spectral differences between the  $T_1$  and  $2xT_1$  state suggests that significant electronic coupling occurs in the transition dipole moments of aligned pentacene triplets.<sup>42</sup> This coupling results from the close proximity of the two pentacenes and the highly planar geometry resulting from conjugation. While direct conjugation of the two pentacenes promotes efficient subpicosecond singlet fission, the resulting fast triplet lifetimes are detrimental to potential applications based on exciton harvesting. Furthermore, while there is no evidence to suggest any parasitic processes that compete with iSF, spectral differences between one and two triplets preclude a direct yield determination to support the observation of a conserved ground-state bleach signal during the conversion of singlets to triplets. To address these issues, we turn to **BP1** and **BP2**.

**Comparison of BP0 to BP1 and BP2.** In **BP1** and **BP2**, the proximity of the pentacenes is decreased by adding phenylene spacers. Inclusion of the spacers also results in additional rotational axes. Notably, this structural change negligibly affects the singlet state; the optical extinction coefficients and low-energy spectral positions are nearly identical in the three bipentacene compounds (Figure 2). Differences in the high-energy optical absorption features upon addition of the phenylene spacers likely result from differences in the symmetry of the molecules. Further investigation into the origin of these high-energy peaks in **BP0** is still underway.

Despite the similarities in the singlet states, systematically decreasing fission rates relative to **BP0** are observed with increasing spacer length. The ultrafast transient absorption data of **BP1** and **BP2** are qualitatively very similar to **BP0**, differing primarily by the rates of the singlet to triplet conversion. The raw transient absorption data are shown in Supporting Information. Because of more complex dynamics in the triplet manifold (discussed below), the singlet fission rate is best determined by time-resolved photoluminescence. We find that the fission rate constant ( $\tau_{\text{SF}}$ ) evolves from 0.7 ps in **BP0** to 20 ps in **BP1** and to 220 ps in **BP2** (Figure 4). Details of the analysis are described in Supporting Information. While an order of magnitude decrease in the rate per phenylene spacer might seem dramatic, the long singlet exciton lifetime of **TPc** (13 ns) allows for effectively quantitative fission processes even in the long spacer limit.<sup>33</sup> On the basis of the emission dynamics, if we assume that singlet fission competes with the same intrinsic singlet decay rate as **TPc**, the iSF yields are calculated to be 199.9%, 199.7%, and 196.7% for **BP0**, **BP1**, and **BP2**. These values are consistent with the measured PL quantum yields (1.6%, 4.4%, and 5.0%, respectively; details in

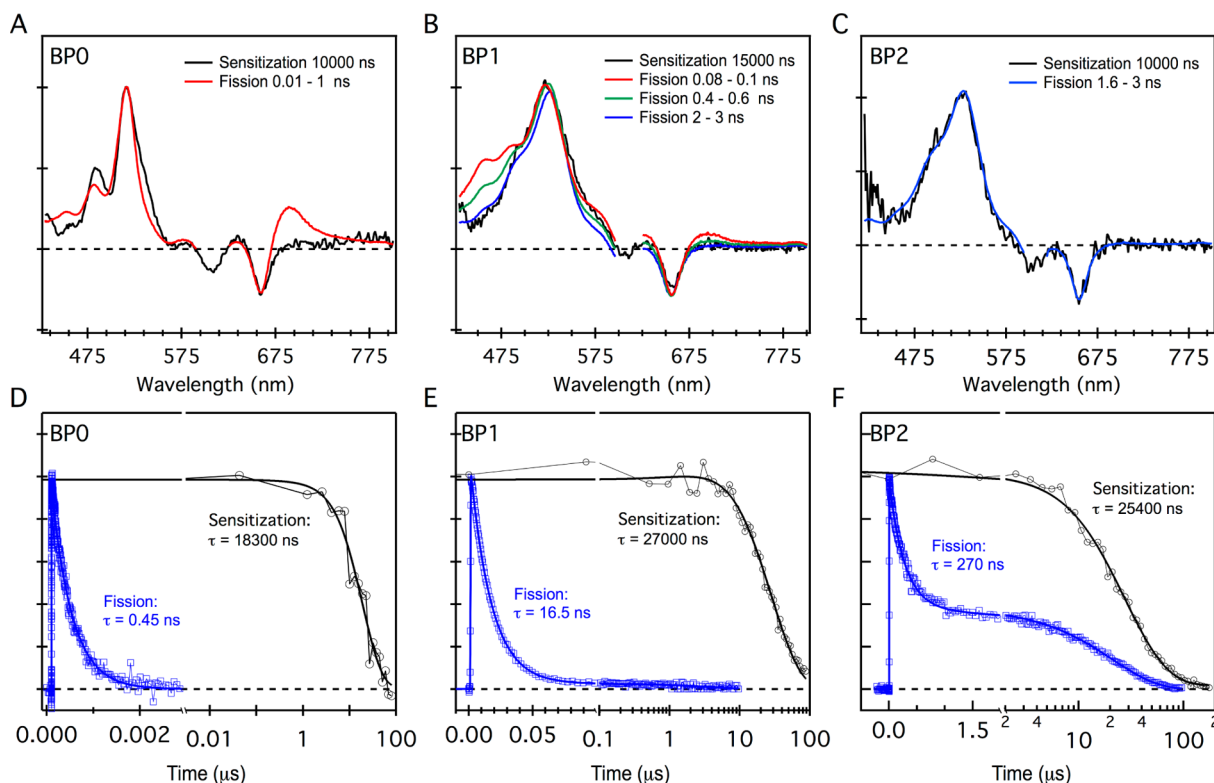


**Figure 5.** Comparison of spectra (A–C) and lifetimes (D–F) of triplets obtained from singlet fission, which produces two triplets, and triplet photosensitization, which populates just one triplet.

Supporting Information) when we account for emission from fluorescent impurities (1–4%) that are readily seen in time-resolved photoluminescence measurements.

When the design of the three chromophores is considered, the varying separation between **BP0**, **BP1**, and **BP2** reduces the proximity of the two triplets localized on each pentacene moiety, in addition to slowing down the rate of triplet–triplet recombination. Furthermore, the isolated triplet transitions can be observed when the pentacenes are sufficiently apart, resulting in the convergence of the  $T_1$  and  $2xT_1$  transient spectra. In **BP1**, the triplet PIA spectrum resembles **BP0** immediately after excitation, and differs from the sensitization spectrum on the low-energy side of the bleach (680 nm, Figure 5B). This state evolves over the next  $\sim 1$  ns to match the single-triplet state, indicating that fully independent, uncoupled triplets are produced. Notably, the  $2xT_1$  lifetime (16.5 ns) is much shorter than the single-triplet lifetime (27  $\mu$ s) obtained from photosensitization (Figure 5E). In **BP2**, however, the  $2xT_1$  state immediately produced by iSF is spectrally indistinguishable from the single-triplet spectrum, indicating that singlet fission directly produces decoupled triplets (Figure 5C). In the triplet recombination dynamics, a bimodal distribution is observed, with a relatively fast component exhibiting a lifetime of  $\sim 270$  ns and a long-lived component approaching that of the individual triplet lifetime (25  $\mu$ s). The nature of this biexponential decay is likely related to conformational changes that occur within the molecule on long time scales, as it is independent of **BP2** concentration but weakly solvent-dependent (Figure S1.7, Supporting Information).

The differences in the transient optical spectra produced by singlet fission, which results from direct optical excitation, and triplet photosensitization, in which a single triplet is transferred

to the molecule, are crucial to our assignment of intramolecular singlet fission. In the singlet fission process summarized in Figure 6, direct optical excitation of the bipentacene derivatives results in a delocalized singlet state, which undergoes a small amount of photoluminescence (<5%) before decaying to produce a triplet pair ( $2xT_1$ ). The two triplets recombine

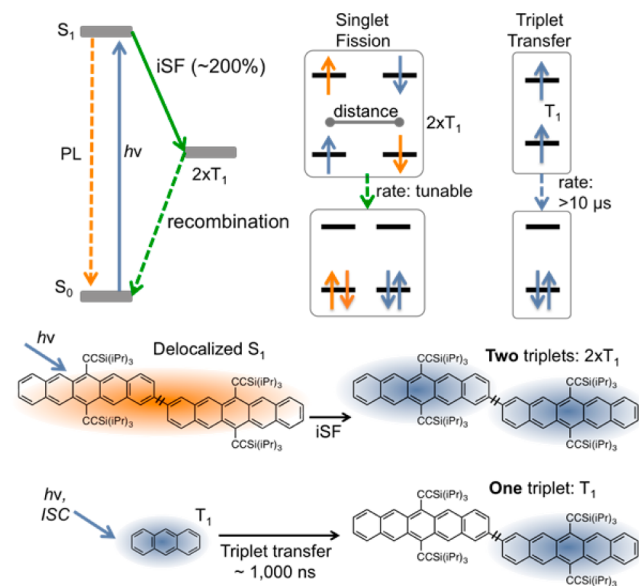


**Figure 6.** Comparison of bipentacenes under optical excitation, which results in ultrafast intramolecular singlet fission (iSF) producing a triplet pair that recombines on time scales varying from 0.45 ns up to 270 ns; and bipentacenes excited by photosensitization triplet transfer with anthracene to produce a single, long-lived triplet.

with a time constant ranging from 0.5 ns (**BP0**) to  $\sim 0.3 \mu\text{s}$  (**BP2**). During sensitization experiments, triplet energy transfer generates an individual triplet that decays to the ground state via a spin-forbidden relaxation process on a much slower time scale ( $>10 \mu\text{s}$ ).

**Singlet Fission Yield Determination.** In all three bipentacene derivatives, the rapid conversion of singlets into the triplet pair in dilute solution is assigned to the dynamical process of iSF, with a triplet yield approaching 200% that matches the best xSF solid-state systems. We base this on the fact that the singlet decay rate is orders of magnitude faster than the corresponding singlet lifetime of **TPc**, and no other species besides the singlet and triplet features are identified in the transient absorption spectra. Furthermore, radiative losses, measured by steady-state photoluminescence, are minimal in these molecules (details in Supporting Information). Similarly, we can rule out the presence of additional nonradiative decay channels, which have been shown to disrupt the correlation between the singlet decay and triplet rise.<sup>20</sup>

An additional way to determine the yield is through quantification of the ground-state bleach (GSB). While quantitative xSF has been shown to produce twice the GSB after singlet fission due to production of two triplet excitons, in the case of the bipentacenes reported here, the conjugation of the chromophores results in a different situation.<sup>43</sup> The DFT calculations included in Supporting Information and discussed earlier reveal extensive delocalization of the singlet exciton, even in the case of **BP2**. Therefore, we expect the singlet exciton to bleach both pentacenes in the dimers. Indeed, transient absorption experiments controlling for photon flux and solution optical density reveal that, even for **BP2**, both pentacenes in the dimer are bleached by the singlet exciton (section SIIA, Supporting Information).<sup>33</sup>

Because the singlet exciton fully bleaches the ground-state transitions, in the case of quantitative iSF, we expect to observe a constant bleach during fission. Using a modified version of the bleach addition method pioneered by Eaton et al.,<sup>43</sup> we find no change in the bleach before and after iSF in any of the three bipentacenes (section SIIA, Supporting Information). Our analysis suggests that while the bleach signal may appear to reduce (**BP0**), remain constant (**BP1**), or intensify (**BP2**) during singlet fission, in the case of dimers studied here, this perceived change is merely a result of overlap between GSB and PIA from the singlet and/or triplet excitons and not due to a change in population of excited chromophores.<sup>28</sup>

In **BP2**, the similarity of the  $T_1$  and  $2xT_1$  spectra allows for yet another iSF yield determination, in this case utilizing sensitization experiments to determine the triplet excited-state absorption extinction coefficient. The iSF yield can then be directly computed from TAS by use of the Beer–Lambert law. In **BP2**, the iSF yield is determined to be  $201\% \pm 15\%$ , consistent with our estimates of the maximum yield from the singlet decay rate of **TPc** monomer (196.7%). Our procedure (detailed in Supporting Information) uses **TPc** as an internal standard for a determination of both the singlet and triplet concentration; that is, the calculation does not rely on literature values for the triplet extinction coefficient of the sensitizer. Crucially, this method is valid only in cases where the spectrum of the two triplets, produced by fission, matches that of a single triplet produced from sensitization. This result supports the assertion that no additional loss channels exist in these compounds. Furthermore, this result confirms that the constant bleach during fission is indeed indicative of near-quantitative

singlet fission yields. This yield information, as well as iSF and triplet decay time constants, is summarized in Table 1.

**Table 1. Summary of Relevant Singlet Fission Time Constants, Triplet Lifetime, and Triplet Yields for Compounds Discussed in This Work**

compd	$\tau_{\text{SF}}$	$\tau_{\text{triplet decay}}$ (ns)	triplet yield (%)
<b>BP0</b>	760 fs	0.45	$\sim 200$
<b>BP1</b>	20 ps	16.5	$\sim 200$
<b>BP2</b>	220 ps	270 <sup>a</sup>	$\sim 200$

<sup>a</sup>It should be noted that **BP2** has a biexponential triplet decay, as discussed above, and the lifetime quoted is the shorter time constant.

We note that the distinct  $2xT_1$  spectra observed after iSF in **BP0** and at early times in **BP1** are a unique feature of iSF molecules with little separation between chromophores. We postulate that spectral shifting between  $T_1$  and  $2xT_1$  occurs because the triplet transition dipole moments are aligned and in close proximity.<sup>42</sup> This alignment occurs as long as the pentacene units are relatively planar; in **BP1**, the triplets live long enough for the molecular backbone to distort to a nonplanar geometry. The electronic coupling observed here should not be confused with strongly coupled multiexciton states (such as the ME state that couples the singlet and triplet manifold). In both **BP0** and **BP1**, we are observing singlet fission to produce independent triplet excitons, in which one or both excitons may be harvested for various applications of optoelectronic materials.

## CONCLUSIONS

We have designed and synthesized **BP0**, **BP1**, and **BP2** as materials that can be used to understand how the excited-state dynamics are dependent on molecular connectivity of the SF chromophores. Calculations demonstrate that iSF is energetically feasible in these molecules due to a localization of triplets on each pentacene unit, resulting from favorable exchange energy interactions. Unlike pentacene monomers, which depend on intermolecular interactions for singlet fission, these bipentacenes yield two triplets independent of intermolecular coupling. This intramolecular process is important because it is independent of packing order and can be observed in solution. Thus, the materials have potential to be studied and exploited in noncrystalline media, by use of high-throughput processing techniques. We experimentally demonstrated that these molecules undergo quantitative, ultrafast intramolecular singlet fission using transient absorption and time-resolved photoluminescence spectroscopy, similar to observations reported during the review of this paper.<sup>28</sup> Triplet sensitization was used to determine the nature of the observed transients and to elucidate the distinct triplet pair recombination dynamics. Similar to the other recently reported pentacene dimer system, we observe fast, high-yielding iSF.<sup>28</sup> However, in contrast, we employ progressively longer spacers to extend triplet pair lifetimes. In the limit of a two-phenylene spacer bridge, we achieve triplet pair lifetimes as long as 270 ns, which may enable harvesting of two electron–hole pairs for devices with enhanced photocurrents. Currently, we are exploring the application of bipentacenes in devices, as well as SF of these molecules in the solid state.

## ■ EXPERIMENTAL SECTION

**Synthesis and Materials.** All commercially available reagents and solvents were used as received, unless otherwise noted. Anhydrous solvents were obtained from a Schlenk manifold with purification columns packed with activated alumina and supported copper catalyst (Glass Contour, Irvine, CA). All reactions were carried out under argon, unless otherwise noted.  $^1\text{H}$  and  $^{13}\text{C}$  NMR spectra were recorded at 300 K on Bruker DRX400 (400 MHz) or Bruker DRX500 (500 MHz) Fourier transform (FT) NMR spectrometers. High-resolution mass spectra were recorded on a JEOL JMSHX110A/110A tandem mass spectrometer. Full synthetic details are provided in Supporting Information.

**Triplet Photosensitization.** Triplets were generated by excitation of an excess of anthracene, which undergoes intersystem crossing (ISC), and were subsequently transferred via diffusional collisions to bipentacene. In this way, a single triplet could be transferred to the bipentacene, in direct contrast to optical excitation, which produced a triplet pair in the case of SF materials. Then the solution was optically probed to reveal the induced absorption spectrum of the triplet and the native triplet lifetime.

**Ultrafast Photoluminescence Spectroscopy.** Ultrafast photoluminescence decay kinetics were measured by the upconversion technique. Briefly, a 100  $\mu\text{M}$  solution in chloroform was resonantly excited with a 100 fs laser pulse tuned to 560 nm. The spontaneous emission was collected by use of a 610 nm long pass filter and mixed with a second “gate” pulse in a nonlinear crystal in a geometry optimized for sum frequency generation. The magnitude of the unconverted optical signal was proportional to the instantaneous photoluminescence intensity and was detected as a function of delay between the excitation and gate pulses. The spectral resolution of this measurement was  $\sim 10$  nm, and the time resolution of this method was measured to be  $\sim 250$  fs by cross-correlating scattered light from the excitation pulse with the optical gate pulse.

## ■ ASSOCIATED CONTENT

### ■ Supporting Information

(I) Text and eight figures describing transient absorption spectroscopy; (II) text and six figures describing singlet fission yield determination; (III) text and five figures describing UV-vis, photoluminescence, and PL quantum yield; (IV) text, five figures, and one table describing computational methods; (V) text and graphics describing synthetic information; (VI) eight NMR spectra; (VII) text and one table describing single-crystal X-ray diffraction; (Appendix A) geometry optimization of  $S_0$  states. The Supporting Information is available free of charge on the ACS Publications website at DOI: 10.1021/jacs.5b04986.

## ■ AUTHOR INFORMATION

### Corresponding Authors

\*E-mail mls2064@columbia.edu.

\*E-mail msfeir@bnl.gov.

\*E-mail lcampos@columbia.edu.

### Present Address

<sup>||</sup>(J.X.) Department of Chemistry, Wuhan Institute of Technology, Wuhan, China.

### Notes

The authors declare no competing financial interest.

## ■ ACKNOWLEDGMENTS

This work was funded by the NSF Career Award (DMR-1351293), ACS Petroleum Research Fund, 3M Non-Tenured Faculty Award, and Cottrell Scholar Award. S.N.S., A.B.P., and B.C. thank the NSF for GRFP (DGE 11-44155). X.Y.Z. acknowledges support by the NSF, Grant 1321405. J.Z.L.

thanks A\*STAR for funding. Research was carried out in part at the Center for Functional Nanomaterials, Brookhaven National Laboratory, and in the Chemistry Department, Brookhaven National Laboratory, which is supported by the U.S. Department of Energy, Office of Basic Energy Sciences, under Contract DE-AC02-98CH10886, which also supports the LEAF Facility of the BNL Accelerator Center for Energy Research. SCXRD was performed in the Shared Materials Characterization Laboratory at Columbia University. X.R. thanks the Air Force Office of Scientific Research for support (AFOSR Award No. FA9550-14-1-0381). We are grateful to the Nuckolls lab for use of their computing cluster and UV-vis spectrophotometer.

## ■ REFERENCES

- (1) Green, M. A. *Prog. Photovoltaics* **2001**, *9*, 123.
- (2) Nozik, A. J. *Phys. E* **2002**, *14*, 115.
- (3) Shockley, W.; Queisser, H. J. *J. Appl. Phys.* **1961**, *32*, 510.
- (4) Singh, S.; Jones, W. J.; Siebrand, W.; Stoicheff, B. P.; Schneider, W. G. *J. Chem. Phys.* **1965**, *42*, 330.
- (5) Congreve, D. N.; Lee, J.; Thompson, N. J.; Hontz, E.; Yost, S. R.; Reuswig, P. D.; Bahlke, M. E.; Reineke, S.; Van Voorhis, T.; Baldo, M. A. *Science* **2013**, *340*, 334.
- (6) Hanna, M. C.; Nozik, A. J. *J. Appl. Phys.* **2006**, *100*, No. 074510.
- (7) Lee, J.; Jadhav, P.; Baldo, M. A. *Appl. Phys. Lett.* **2009**, *95*, No. 033301.
- (8) Lee, J.; Jadhav, P.; Reuswig, P. D.; Yost, S. R.; Thompson, N. J.; Congreve, D. N.; Hontz, E.; Van Voorhis, T.; Baldo, M. A. *Acc. Chem. Res.* **2013**, *46*, 1300.
- (9) Yost, S. R.; Lee, J.; Wilson, M. W. B.; Wu, T.; McMahon, D. P.; Parkhurst, R. R.; Thompson, N. J.; Congreve, D. N.; Rao, A.; Johnson, K.; Sfeir, M. Y.; Bawendi, M. G.; Swager, T. M.; Friend, R. H.; Baldo, M. A.; Van Voorhis, T. *Nat. Chem.* **2014**, *6*, 492.
- (10) Chan, W.-L.; Ligges, M.; Jailaubekov, A.; Kaake, L.; Miaja-Avila, L.; Zhu, X.-Y. *Science* **2011**, *334*, 1541.
- (11) Chan, W.-L.; Berkelbach, T. C.; Provorse, M. R.; Monahan, N. R.; Tritsch, J. R.; Hybertsen, M. S.; Reichman, D. R.; Gao, J.; Zhu, X. Y. *Acc. Chem. Res.* **2013**, *46*, 1321.
- (12) Zeng, T.; Hoffmann, R.; Ananth, N. *J. Am. Chem. Soc.* **2014**, *136*, 5755.
- (13) Pensack, R. D.; Tilley, A. J.; Parkin, S. R.; Lee, T. S.; Payne, M. M.; Gao, D.; Jahnke, A. A.; Oblinsky, D.; Li, P.-F.; Anthony, J. E.; Seferos, D. S.; Scholes, G. D. *J. Am. Chem. Soc.* **2015**, *137*, 6790.
- (14) Piland, G. B.; Bardeen, C. J. *J. Phys. Chem. Lett.* **2015**, 1841.
- (15) Roberts, S. T.; McAnally, R. E.; Mastron, J. N.; Webber, D. H.; Whited, M. T.; Brutchey, R. L.; Thompson, M. E.; Bradforth, S. E. *J. Am. Chem. Soc.* **2012**, *134*, 6388.
- (16) Mastron, J. N.; Roberts, S. T.; McAnally, R. E.; Thompson, M. E.; Bradforth, S. E. *J. Phys. Chem. B* **2013**, *117*, 15519.
- (17) Gradinaru, C. C.; Kennis, J. T. M.; Papagiannakis, E.; van Stokkum, I. H. M.; Cogdell, R. J.; Fleming, G. R.; Niederman, R. A.; van Grondelle, R. *Proc. Natl. Acad. Sci. U.S.A.* **2001**, *98*, 2364.
- (18) Musser, A. J.; Al-Hashimi, M.; Maiuri, M.; Brida, D.; Heeney, M.; Cerullo, G.; Friend, R. H.; Clark, J. *J. Am. Chem. Soc.* **2013**, *135*, 12747.
- (19) Trinh, M. T.; Zhong, Y.; Chen, Q.; Schiros, T.; Jockusch, S.; Sfeir, M. Y.; Steigerwald, M.; Nuckolls, C.; Zhu, X. *J. Phys. Chem. C* **2015**, *119*, 1312.
- (20) Busby, E.; Xia, J.; Wu, Q.; Low, J. Z.; Rong, R.; Miller, J. R.; Zhu, X.-Y.; Campos, L. M.; Sfeir, M. Y. *Nat. Mater.* **2014**, *14*, 426.
- (21) Varnavski, O.; Abeyasinghe, N.; Aragón, J.; Serrano-Pérez, J. J.; Ortí, E.; López Navarrete, J. T.; Takimiya, K.; Casanova, D.; Casado, J.; Goodson, T. *J. Phys. Chem. Lett.* **2015**, *6*, 1375.
- (22) Burdett, J. J.; Bardeen, C. J. *Acc. Chem. Res.* **2013**, *46*, 1312.
- (23) Vallett, P. J.; Snyder, J. L.; Damrauer, N. H. *J. Phys. Chem. A* **2013**, *117*, 10824.

- (24) Müller, A. M.; Avlasevich, Y. S.; Schoeller, W. W.; Müllen, K.; Bardeen, C. J. *J. Am. Chem. Soc.* **2007**, *129*, 14240.
- (25) Smith, M. B. M. *J. Chem. Rev.* **2010**, *110*, 6891.
- (26) Greyson, E. C.; Vura-Weis, J.; Michl, J.; Ratner, M. A. *J. Phys. Chem. B* **2010**, *114*, 14168.
- (27) Smith, M. B.; Michl, J. *Annu. Rev. Phys. Chem.* **2013**, *64*, 361.
- (28) Zirzmeier, J.; Lehnher, D.; Coto, P. B.; Chernick, E. T.; Casillas, R.; Basel, B. S.; Thoss, M.; Tykwinski, R. R.; Guldi, D. M. *Proc. Natl. Acad. Sci. U.S.A.* **2015**, *112*, 5325.
- (29) Greyson, E. C.; Stepp, B. R.; Chen, X.; Schwerin, A. F.; Paci, I.; Smith, M. B.; Akdag, A.; Johnson, J. C.; Nozik, A. J.; Michl, J.; Ratner, M. A. *J. Phys. Chem. B* **2009**, *114*, 14223.
- (30) Fudickar, W.; Linker, T. *J. Am. Chem. Soc.* **2012**, *134*, 15071.
- (31) Smith, M. B.; Michl, J. *Annu. Rev. Phys. Chem.* **2013**, *64*, 361.
- (32) Lehnher, D.; Tykwinski, R. R. *Materials* **2010**, *3*, 2772.
- (33) Walker, B. J.; Musser, A. J.; Beljonne, D.; Friend, R. H. *Nat. Chem.* **2013**, *5*, 1019.
- (34) Snellenburg, J. J. L.; S, P.; Seger, R.; Mullen, K. M.; van Stokum, I. H. M. *J. Stat. Software* **2012**, *49*, 1.
- (35) Poletayev, A. D.; Clark, J.; Wilson, M. W. B.; Rao, A.; Makino, Y.; Hotta, S.; Friend, R. H. *Adv. Mater.* **2014**, *26*, 919.
- (36) Bensasson, R.; Land, E. J. *Trans. Faraday Soc.* **1971**, *67*, 1904.
- (37) Turro, N. J. *Modern Molecular Photochemistry*; University Science Books: Sausalito, CA, 1991.
- (38) Rettig, W. *Angew. Chem., Int. Ed.* **1986**, *25*, 971.
- (39) Rettig, W. *J. Mol. Struct.* **1982**, *84*, 303.
- (40) Grabowski, Z. R.; Rotkiewicz, K.; Siemiarz, A. *J. Lumin.* **1979**, *18–19* (Part 1), 420.
- (41) Fery-Forgues, S.; Fayet, J.-P.; Lopez, A. J. *Photochem. Photobiol., A* **1993**, *70*, 229.
- (42) Marciniak, H.; Pugliesi, I.; Nickel, B.; Lochbrunner, S. *Phys. Rev. B* **2009**, *79*, No. 235318.
- (43) Eaton, S. W.; Shoer, L. E.; Karlen, S. D.; Dyar, S. M.; Margulies, E. A.; Veldkamp, B. S.; Ramanan, C.; Hartzler, D. A.; Savikhin, S.; Marks, T. J.; Wasielewski, M. R. *J. Am. Chem. Soc.* **2013**, *135*, 14701.